

Experimental study of weak intersystem lines and related strong persistent lines of Ne II

J. M. Bridges and W. L. Wiese

National Institute of Standards and Technology, Gaithersburg, Maryland 20899, USA

(Received 27 March 2007; published 31 August 2007)

We operated a high-current hollow cathode discharge in pure neon at pressures from 93 to 173 Pa and measured the branching fractions of Ne II emission lines originating from several $2p^5 3p$, $3d$, and $4f$ levels, for which lifetime data were available in the literature. This allowed the determination of transition probabilities for all downward transitions, which included a number of weak intersystem lines. We focused our study on these weak lines, using care to assure correct identifications and accurate intensity measurements, in spite of the presence of much stronger other lines in their vicinity. In contrast to an earlier experiment, we achieved close agreement with a recent multiconfiguration Hartree-Fock calculation.

DOI: [10.1103/PhysRevA.76.022513](https://doi.org/10.1103/PhysRevA.76.022513)

PACS number(s): 32.70.-n

I. INTRODUCTION

The spectrum of Ne II provides an interesting test case for the determination of atomic transition probabilities and has thus been the subject of several recent theoretical [1–6] and experimental [7–9] studies. The interest was further stimulated by large discrepancies for the weak intersystem lines between the advanced configuration-interaction calculations of Blackford and Hibbert [6] and the high-current hollow-cathode experiment of Griesmann *et al.* [7]. Recent experiments [8,9] focused on the strong LS -allowed $3s$ - $3p$ and $3p$ - $3d$ transitions and on a few $3d$ - $4f$ transitions, but did not include intersystem lines, while new advanced calculations, especially [2,3,5] have been much more extensive and again included many intersystem lines, producing still different results.

The differences between the various calculations and experiments have now narrowed appreciably for the strong LS -allowed lines and are in many cases in the 10%–20% range. However, for the intersystem lines, most of which are weaker, sometimes by several orders of magnitude, major differences remained. We have therefore made a special effort to obtain reliable results for them, which was the main goal of this experiment.

II. EXPERIMENTAL METHOD

(a) Source: We used a high-current hollow cathode discharge of the type developed by Danzmann *et al.* [10]. The cathode insert was a hollow copper cylinder, 60 mm long, with an 8 mm inner diameter. The source was operated in pure neon. Pressures in the range of 93–173 Pa (0.7–1.3 Torr) were found to give the optimum conditions for strong Ne II line emission when the source was operated at a current of 1.5 A. At higher currents, the source was unstable, but at the above cited conditions, the sputtering rate was sufficiently low that the hollow cathode ran in a stable mode. Also, reproducible intensity readings were obtained for the weakest intersystem lines.

(b) Spectral recording: Using a spherical mirror, we imaged the light source onto the entrance slit of a Czerny-Turner monochromator of 2 m focal length. We recorded the spectral data primarily with a CCD detector, with a spectral resolution of about 0.012 nm. Some data also were taken

with a photomultiplier tube, using an exit slit. When data were taken with both detectors, good agreement was obtained for the relative line intensities.

By monitoring the radiance of a strong Ne II line we checked the long-term stability of the source. Within 15 min, the time needed to record data for all lines of a typical multiplet, no significant variation in the output was found. Each line was recorded at least three times, and the standard deviations of the mean values were in the range of 1%–5%. We set the width of the entrance slit at 30 μm , so that the main part of the intensity of a spectral line extended over four to five adjacent pixels. When we used the photomultiplier, we also set the exit slit at 30 μm . The total line intensities were obtained by fitting Gaussian curves to the line profiles, which provided an excellent fit to the observed line shapes under our experimental conditions. The full width at half maximum was 0.012 nm for all lines, due predominantly to instrumental broadening. For some well-isolated lines, intensities were also obtained by summing the signals in the pixels. This produced essentially the same results for the relative line intensities. For weak lines, considerable care had to be taken to assure their correct identification. Strong lines in their vicinity were identified and straight-line fits were established for pixel number versus wavelength, from which the wavelengths of the weak lines were ascertained. In a few cases, the lines of interest were significantly blended with other lines, but such pairs could be fitted to two blended Gaussian curves and the area of each line could be determined. However, when the weak line was blended with a much stronger line, an accurate measurement was not possible. For some very weak lines that we attempted to measure, no signal was observed. But in some of these cases, an upper limit for the transition probability was determined by estimating what size feature could be positively identified at that wavelength. The minimum value for this estimate was limited by the dark current variations in the pixels.

(c) Calibration of spectral response: The transitions we studied are located in the near ultraviolet and visible regions. We used a calibrated tungsten strip lamp for wavelengths greater than 400 nm and an argon mini arc for wavelengths below 400 nm as our standards of spectral radiance. In the ultraviolet region the tungsten strip lamp signals rapidly decrease toward shorter wavelengths, and since the detector is more sensitive at longer wavelengths, scattered light could become a major problem if the strip lamp would be used.

TABLE I. Transition probabilities (in 10^8 s^{-1}) for some $3s$ - $3p$ lines and comparisons with other experimental and theoretical results.

Transition and upper level lifetime τ	Wavelength (nm)	Experiments				Calculations		
		This Work	Griesmann <i>et al.</i> [7]	Del Val <i>et al.</i> [8]	Djenize <i>et al.</i> [9]	Froese Fischer and Tachiev [2]	Zheng <i>et al.</i> [4]	Froese Fischer and Ralchenko [5]
$3s^2 P_{1/2} - 3p^2 P_{3/2}^o$	339.280	$0.390 \pm 10\%$	0.396	0.415	...	0.3929	0.309	0.3761
$3s^2 P_{3/2} - 3p^2 P_{3/2}^o$	332.374	$1.363 \pm 10\%$	1.350	...	1.45	1.383	1.623	1.4036
$3s^4 P_{1/2} - 3p^2 P_{3/2}^o$	292.161	$0.00055 \pm 14\%$	0.0023	0.000466	...	0.00021
$3s^4 P_{5/2} - 3p^2 P_{3/2}^o$	285.352	$0.00060 \pm 14\%$	0.0030	0.000573	...	0.00017
$\tau = 5.7 \text{ ns}$								
$3s^2 P_{1/2} - 3p^2 D_{3/2}^o$	372.711	$0.943 \pm 11\%$	0.870	0.911	1.26	1.055	1.16	1.0581
$3s^2 P_{3/2} - 3p^2 D_{3/2}^o$	364.393	$0.280 \pm 11\%$	0.289	0.501	...	0.3337	0.247	0.3185
$3s^4 P_{1/2} - 3p^2 D_{3/2}^o$	316.618	$0.00385 \pm 19\%$	0.0198	0.003988	...	0.00422
$3s^4 P_{3/2} - 3p^2 D_{3/2}^o$	313.648	$0.00229 \pm 18\%$	0.0123	0.00265	...	0.00287
$\tau = 8.13 \text{ ns}$								
$3s^2 P_{3/2} - 3p^2 D_{5/2}^o$	371.308	$1.230 \pm 9\%$	1.121	1.041	...	1.374	1.40	1.3616
$3s^4 P_{3/2} - 3p^2 D_{5/2}^o$	318.758	$0.0138 \pm 13\%$	0.0925	0.0145	...	0.01536
$3s^4 P_{5/2} - 3p^2 D_{5/2}^o$	313.582	^a	0.0388	0.00575	...	0.00595
$\tau = 8.0 \text{ ns}$								
$3s^4 P_{1/2} - 3p^4 S_{3/2}^o$	302.886	$0.401 \pm 10\%$	0.420	...	0.61	0.454	0.398	0.4528
$3s^4 P_{3/2} - 3p^4 S_{3/2}^o$	300.167	$0.715 \pm 10\%$	0.763	...	0.80	0.842	0.813	0.8348
$3s^4 P_{5/2} - 3p^4 S_{3/2}^o$	295.573	$0.942 \pm 10\%$	0.967	1.12	1.265	1.1119
$3s^2 P_{1/2} - 3p^4 S_{3/2}^o$	353.826	< 0.0017	0.0043	0.000627	...	0.00031
$3s^2 P_{3/2} - 3p^4 S_{3/2}^o$	346.321	$0.00028 \pm 25\%$	0.0248	0.000231	...	0.00001
$\tau = 4.85 \text{ ns}$								
$3s^4 P_{1/2} - 3p^4 P_{1/2}^o$	375.125	$0.175 \pm 9\%$	0.157	0.19	...	0.1801	0.208	0.1755
$3s^4 P_{3/2} - 3p^4 P_{1/2}^o$	370.962	$1.006 \pm 9\%$	1.020	1.08	...	1.137	1.07	1.1127
$3s^2 P_{1/2} - 3p^4 P_{1/2}^o$	456.51	< 0.0005	0.0053	0.00005	...	0.00003
$\tau = 8.44 \text{ ns}$								
$3s^4 P_{1/2} - 3p^4 P_{3/2}^o$	377.714	$0.317 \pm 12\%$	0.316	0.376	...	0.4233	0.51	0.4117
$3s^4 P_{3/2} - 3p^4 P_{3/2}^o$	373.494	$0.144 \pm 12\%$	0.147	0.209	...	0.1889	0.168	0.1850
$3s^4 P_{5/2} - 3p^4 P_{3/2}^o$	366.407	$0.549 \pm 12\%$	0.553	0.677	0.74	0.7088	0.596	0.6959
$3s^2 P_{3/2} - 3p^4 P_{3/2}^o$	447.74	< 0.0004	0.0011	0.00	...	0.00000
$\tau = 9.88 \text{ ns}$								
$3s^4 P_{3/2} - 3p^4 P_{5/2}^o$	376.626	$0.280 \pm 9\%$	0.270	0.269	...	0.2952	0.368	0.2871
$3s^4 P_{5/2} - 3p^4 P_{5/2}^o$	369.421	$0.955 \pm 9\%$	0.947	0.751	1.13	1.027	0.904	1.0068
$3s^2 P_{3/2} - 3p^4 P_{5/2}^o$	452.24	< 0.00035	0.0185	(0.00001)	...	0.00001
$\tau = 8.1 \text{ ns}$								

^aBlend (total feature is very weak).

III. DATA ANALYSIS

The integrated detector signals of the spectral lines originating from a common upper level k and ending in various lower levels i were calibrated as discussed above to obtain the correct spectral response and were divided by the photon energy, which yields relative photon fluxes F_{ik} (in photons/s). For a given upper level k , when the signals of complete sets of transitions to all lower levels i could be measured, the

individual fluxes divided by the sum total provided the branching fractions B_{ik} , i.e.,

$$B_{ik} = \frac{F_{ik}}{\sum_i F_{ik}} = \frac{A_{ki}}{\sum_i A_{ki}}.$$

The radiative lifetime τ_k of a level k is the inverse sum of the transition probabilities A_{ki} for all possible downward transi-

TABLE II. Transition probabilities (in 10^8 s^{-1}) for some $3p$ - $3d$ lines and comparisons with other experimental and theoretical results.

Transition and upper level lifetime τ	Wavelength (nm)	Experiments			Calculations			
		This work	Griesmann <i>et al.</i> [7]	Del Val <i>et al.</i> [8]	Djenize <i>et al.</i> [9]	Godefroid and Hibbert [1]	Froese Fischer [3]	Froese Fischer and Ralchenko [5]
$3p^4 P_{5/2}^o - 3d^4 D_{7/2}$	303.446	$2.74 \pm 12\%$	2.70	...	3.10	3.02	2.844	2.827
$3p^4 D_{5/2}^o - 3d^4 D_{7/2}$	336.699	$0.0271 \pm 25\%$	0.0108	0.0322	0.02544	0.0293
$3p^4 D_{7/2}^o - 3d^4 D_{7/2}$	332.916	$0.800 \pm 14\%$	0.858	...	1.00	0.894	0.8885	0.864
$\tau = 2.8 \text{ ns}$								
$3p^4 P_{5/2}^o - 3d^4 F_{7/2}$	289.700	$0.0345 \pm 27\%$	0.0133	5.749×10^{-5}	0.0397
$3p^4 D_{5/2}^o - 3d^4 F_{7/2}$	319.859	$1.257 \pm 11\%$	1.105	1.494	1.554	1.631
$3p^4 D_{7/2}^o - 3d^4 F_{7/2}$	316.443	$0.131 \pm 18\%$	0.0846	0.158	0.1591	0.1574
$3p^2 D_{5/2}^o - 3d^4 F_{7/2}$	336.721	$1.210 \pm 11\%$	1.123	1.09	...	1.789	1.641	1.582
$\tau = 3.86 \text{ ns}$								
$3p^2 D_{5/2}^o - 3d^2 F_{7/2}$	341.769	$0.988 \pm 10\%$	1.20	1.16	1.65	1.493	1.564	1.561
$3p^4 D_{5/2}^o - 3d^2 F_{7/2}$	324.409	$1.034 \pm 8\%$	0.856	1.89	1.704	1.576
$3p^4 D_{7/2}^o - 3d^2 F_{7/2}$	320.897	$0.111 \pm 15\%$	0.0764	0.186	0.1578	0.159
$\tau = 4.7 \text{ ns}$								
$3p^2 D_{3/2}^o - 3d^2 F_{5/2}$	338.842	1.673^a	1.673^a	1.50	1.673	2.296
$3p^2 D_{5/2}^o - 3d^2 F_{5/2}$	333.073	$0.0715 \pm 14\%$	0.0579	0.1046	0.0607
$3p^4 P_{3/2}^o - 3d^2 F_{5/2}$	288.842	$0.0267 \pm 14\%$	0.0109	0.06024	0.0317
$3p^4 D_{3/2}^o - 3d^2 F_{5/2}$	319.086	$0.137 \pm 11\%$	0.104	0.1324	0.166
$3p^4 D_{5/2}^o - 3d^2 F_{5/2}$	316.565	$0.182 \pm 11\%$	0.197	0.3022	0.149
$3p^4 D_{7/2}^o - 3d^2 F_{5/2}$	313.219	$0.0715 \pm 14\%$	0.0467	0.1694	0.0180
$3p^2 S_{1/2}^o - 3d^2 P_{3/2}$	345.661	1.389^a	1.389^a	1.182	1.389	1.316
$3p^2 P_{1/2}^o - 3d^2 P_{3/2}$	364.486	$0.954 \pm 9\%$	1.005	1.268	0.7688	0.808
$3p^2 P_{3/2}^o - 3d^2 P_{3/2}$	362.803	$0.513 \pm 9\%$	0.511	0.357	0.40	...	0.3613	0.478
$3p^2 D_{3/2}^o - 3d^2 P_{3/2}$	331.050	$0.121 \pm 11\%$	0.0747	0.1252	0.0979
$3p^2 D_{5/2}^o - 3d^2 P_{3/2}$	325.542	$0.163 \pm 11\%$	0.117	0.1476	0.103
$3p^4 D_{1/2}^o - 3d^2 P_{3/2}$	313.579	^b	0.122	0.03196	0.0175
$3p^4 D_{5/2}^o - 3d^2 P_{3/2}$	309.754	$0.0319 \pm 14\%$	0.00898	0.03707	0.0095
$3p^4 S_{3/2}^o - 3d^2 P_{3/2}$	347.524	$0.0181 \pm 21\%$	0.0932	0.02102	0.0196

^aNormalized to MCHF result (Ref. [3]). The given uncertainties are for the branching fraction measurements only.

^bBlend (total feature is weak).

tions from this level; that is, $\tau_k = (\sum_i A_{ki})^{-1}$. The branching fractions could thus be used to determine absolute transition probabilities A_{ki} via the relation

$$A_{ki} = \frac{B_{ik}}{\tau_k}.$$

However, this requires that radiative lifetimes are available, which is the case for most of the levels studied [11–24].

We used averages of the available data, analogous to Griesmann *et al.* [7]. But the lifetimes measured by Fink *et al.* [22] were systematically shorter, by about 20%, than the other measurements for the $3s$ and $3p$ levels, and therefore were excluded. Most lifetime data were obtained by beam foil spectroscopy, the phase shift, and the delayed coinci-

dence technique—methods that normally produce nonselective excitation of atomic energy levels, unless special efforts are undertaken to correct for this. Only two $3p$ levels were measured with a cascade-free delayed-coincidence technique using threshold electron excitation [11], while the lifetimes for all other transitions are expected to be systematically slightly too long because of repopulation of the states due to cascading electrons from higher levels. For the $2p^5 3d^2 P_{3/2}$ and the $3d^2 F_{5/2}$ levels, some strong contributing lines are located in the vacuum ultraviolet and could not be measured. In this case, we normalized our branching fraction data to the result for the strongest line obtained from a recent multiconfiguration Hartree-Fock (MCHF) calculation [3]. This very sophisticated calculation was carried out in the dipole length as well as the dipole velocity approximations, and a differ-

TABLE III. Transition probabilities (in 10^8 s^{-1}) for some $3d$ - $4f$ lines and comparison with other experimental and theoretical results.

Transition and upper level lifetime τ	Wavelength (nm)	Experiments		Calculations	
		This work	Del Val <i>et al.</i> [8]	Froese Fischer and Ralchenko [5]	Froese Fischer [3]
$3d^4 D_{7/2} - 4f^2 [4]_{9/2}^o$	409.886	$0.186 \pm 31\%$...	0.2485	0.2320
$3d^4 F_{7/2} - 4f^2 [4]_{9/2}^o$	437.955	$1.98 \pm 30\%$	0.361	2.081	2.070
$\tau = 4.6 \text{ ns}$					
$3d^4 D_{5/2} - 4f^2 [4]_{7/2}^o$	411.239	$0.046 \pm 18\%$...	0.05673	0.05251
$3d^2 D_{5/2} - 4f^2 [4]_{7/2}^o$	429.809	$0.024 \pm 23\%$	0.03402
$3d^4 F_{7/2} - 4f^2 [4]_{7/2}^o$	437.940	^a	0.07101
$3d^4 F_{5/2} - 4f^2 [4]_{7/2}^o$	439.799	$1.56 \pm 15\%$...	1.795	1.843
$3d^2 F_{5/2} - 4f^2 [4]_{7/2}^o$	444.269	$0.166 \pm 15\%$	0.1234
$3d^4 P_{5/2} - 4f^2 [4]_{7/2}^o$	447.159	$0.127 \pm 15\%$	0.1741
$\tau = 5.0 \text{ ns}$					
$3d^4 D_{1/2} - 4f^2 [2]_{3/2}^o$	415.069	$0.997 \pm 31\%$	0.098	0.8103	0.7765
$3d^4 P_{1/2} - 4f^2 [2]_{3/2}^o$	439.631	$0.213 \pm 31\%$	0.1779
$3d^4 F_{3/2} - 4f^2 [2]_{3/2}^o$	443.946	$0.515 \pm 31\%$...	0.4116	0.3310
$3d^2 P_{1/2} - 4f^2 [2]_{3/2}^o$	450.813	$0.776 \pm 31\%$	0.050	0.6417	0.6504
$\tau = 4.0 \text{ ns}$					
$3d^2 P_{3/2} - 4f^2 [2]_{5/2}^o$	458.814	0.270 ^b	...	0.270	0.270
$3d^2 F_{3/2} - 4f^2 [2]_{5/2}^o$	444.644	$0.253 \pm 17\%$...	0.256	0.255
$3d^4 F_{3/2} - 4f^2 [2]_{5/2}^o$	443.925	$0.442 \pm 17\%$...	0.280	0.245
$3d^2 D_{3/2} - 4f^2 [2]_{5/2}^o$	433.983	$0.240 \pm 17\%$...	0.210	0.205
$3d^4 D_{3/2} - 4f^2 [2]_{5/2}^o$	413.369	$0.374 \pm 17\%$...	0.391	0.378

^aBlend, total feature is very weak.^bNormalized to Refs. [3,5] (MCDF results). Lifetime data could not be applied, because not all branches could be measured.

Uncertainties refer to branching fraction measurement only.

ence of only 1.9% was found in the results. Since our main goal is to get accurate results for the weak intersystem lines that are obtained from measured intensity ratios with a strong LS -allowed line, this normalization represents an adequate alternative to lifetime data.

Our emission method requires that the radiation be emitted from an optically thin medium. Therefore, self-absorption checks were always performed for the strong lines. By operating at different discharge currents, the line intensities could be varied over a large range. However, the signal ratio of a strong to a weak line, originating from the same level, will remain constant only when the two lines are both emitted from an optically thin layer. This was the case for all lines we measured, indicating that self-absorption was absent.

IV. RESULTS AND DISCUSSION

We have measured the branching fractions of emission lines from several $3p$, $3d$, and $4f$ levels. We specifically selected levels that fulfilled three conditions: (1) All significant

downward transitions could be measured, (2) the transition probabilities of the contributing weaker intersystem transitions showed substantial disagreements among earlier results, and (3) either radiative lifetimes or reliable theoretical results were available for the strongest lines from these levels that could provide the normalization to the absolute scale.

Tables I–III show our results on an absolute scale and comparisons with other work of the last ten years. We arranged the transitions by upper level in order to facilitate their normalization by available lifetime data, and we applied and averaged published lifetime results [11–24] for this. We also list our uncertainty estimates, in percent. These are the combined uncertainties of our branching fraction measurements and those of the applied lifetime data.

Table I contains the results of our measurements for the LS -allowed as well as the intersystem emission lines from seven $3p$ levels into various $3s$ states. For two of these levels, $3p^2 D_{5/2}$ and $3p^4 P_{5/2}$, lifetimes with threshold excitation have been determined [11], which produces cascade-free results, and these were not averaged with any other results. For these two levels, our results for the strong LS -allowed lines agree within 11% or better with the similar emission mea-

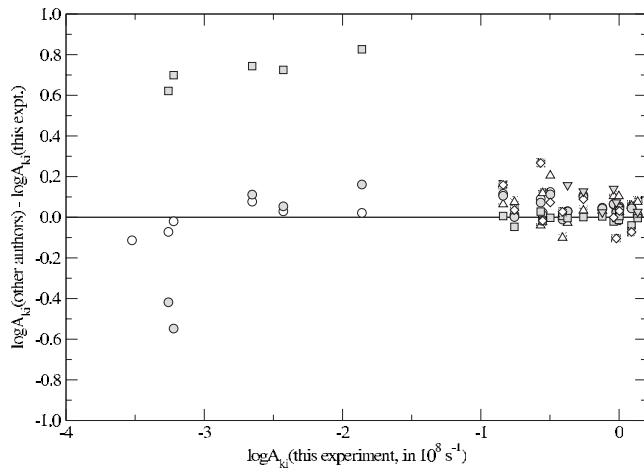


FIG. 1. Comparison of other experimental and theoretical results with our data for $3s$ - $3p$ transitions. The ratios (on a logarithmic scale) with the experiments of Griesmann *et al.* ([7], squares), Del Val *et al.* ([8], diamonds), Djenize *et al.* ([9], triangles) and with the calculations of Froese Fischer and Tachiev ([2], MCHF open circles), and Froese Fischer and Ralchenko ([5], MCDF rescaled, filled-in circles) are plotted versus the A_{ki} of this experiment.

surements by Griesmann *et al.* [7] and the multiconfiguration Hartree Fock (MCHF) calculations by Froese Fischer and Tachiev [2], and the agreement with the other results is also good. Even for a much weaker intersystem line from these levels, our agreement with the MCHF calculations remains good. For the extremely weak line at 452.24 nm, our experiment as well as the MCHF calculations could obtain only rough estimates, which are, however, consistent with one another.

For the lines from the other five $3p$ levels, the situation is similar: For the strong LS -allowed lines, we obtained the best agreement with the experimental data of Griesmann *et al.* [7]. The agreement with the MCHF calculations of Froese Fischer and Tachiev [2] is also good, except for the lines from the $3p^4P_{3/2}$ level, where it is only fair. Our agreement with the other two experiments by Del Val *et al.* [8] and by Djenize *et al.* [9] is not as consistently good as with Griesmann *et al.* [7]. Differences span a range from a few percent to discrepancies exceeding fifty percent.

For the much weaker intersystem lines, our agreement with the MCHF calculations remains good. For three very weak lines, both our experiment and the MCHF calculations can only provide rough estimates, which, however, are qualitatively consistent with each other. These transition probabilities are estimated to be extremely small, while the Griesmann *et al.* results are larger by factors of 3–60.

A graphical comparison of our results with all recent experiments and calculations for the transition probabilities of the $3s$ - $3p$ transitions is shown in Fig. 1. While the data situation is very satisfactory for the strong LS -allowed lines, for the weak intersystem lines our measured data agree closely only with the MCHF calculations of Froese Fischer and Tachiev [2], and—except for the two weakest lines—also with the rescaled MCDF calculations of Froese Fischer and Ralchenko [5]. But we disagree strongly, in a nearly regular

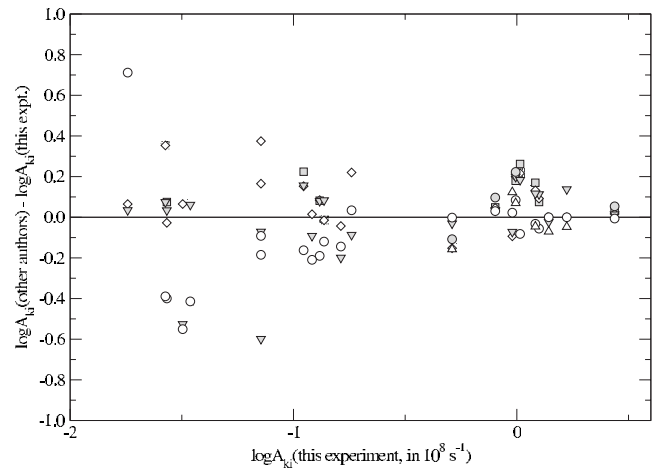


FIG. 2. Comparison of other experimental and theoretical results with our data for $3p$ - $3d$ transitions. The ratios (on a logarithmic scale) with the experiments of Griesmann *et al.* ([7], open circles), Del Val *et al.* ([8], triangles) and Djenize *et al.* ([9], filled circles), and with the calculations of Froese Fischer ([3], MCHF, diamonds), Froese Fischer and Ralchenko ([5], MCDF, inverted triangles) and Godefroid and Hibbert ([1], CIV 3 code) are plotted versus the $A(ki)$ of this experiment.

manner, with all experimental data of Griesmann *et al.* [7] for these weak lines. The cause of our discrepancies with the similar emission experiment of Griesmann *et al.* remains a puzzle. Possible reasons are a normalization error for the intensities of the weak $3s$ - $3p$ transitions, or misidentifications by Griesmann *et al.* of these weak features, which are often very close to other, much stronger Ne II transitions.

The situation is similar for the $3p$ - $3d$ and $3d$ - $4f$ transitions, which are presented in Tables II and III, and in Fig. 2. Our experimental results are, on average, slightly smaller than the calculated ones. This systematic difference is most likely due to unrecognized cascading effects in the lifetime measurements used for normalization, which always make the lifetimes appear longer, or the transition probabilities smaller. As was already mentioned, for the $3d^2P_{3/2}$ and the $3d^2F_{5/2}$ levels we could not measure complete sets of emission lines and therefore could not apply lifetime data. We therefore normalized our branching fractions for the strongest line emitted from these levels to the values from the MCHF calculations. Table II, as well as Fig. 2, show that for the weak intersystem lines, large and apparently random differences occur between our data, the Griesmann *et al.* [7] results, and some MCHF and MCDF values.

Finally, Table III exhibits good-to-fair agreement between our results and the MCDF data of Froese Fischer and Ralchenko [5] for the $3d$ - $4f$ transitions we measured, but poor agreement with the measurements of Del Val *et al.* [8] for all three lines they determined.

As we noted at the outset, our main goal was to determine accurate data for the usually weak intersystem lines in the $3s$ - $3p$ and $3p$ - $3d$ transition arrays of Ne II. Our measurements provide the first experimental test for the extensive MCHF and MCDF calculations of Froese Fischer and co-workers [2,3,5]. As is usual for such complex calculations, they do not by themselves allow accurate uncertainty esti-

mates. The data for the weak intersystem lines are especially sensitive to inaccuracies in the calculations. Thus, even the relatively few intersystem lines measured by us provide a fairly critical test for the quality of the new calculations. Indeed, we found consistently good agreement with these calculations for each of the tested lines. Thus, our experiment provides strong support for the new advanced theoret-

ical work and contributes to a substantial improvement in the data situation for the weak lines of Ne II.

ACKNOWLEDGMENT

The authors are grateful to Charlotte Froese Fischer and Yuri Ralchenko for valuable discussions and their interest.

-
- [1] M. R. Godefroid and A. Hibbert, *Mol. Phys.* **98**, 1009 (2000).
 - [2] Ch. Froese Fischer and G. Tachiev, *At. Data Nucl. Data Tables* **87**, 1 (2004).
 - [3] Ch. Froese Fischer, MCHF/MCDHF Collection, <http://atoms.vuse.vanderbilt.edu/>
 - [4] N. W. Zheng and T. Wang, *Spectrochim. Acta, Part B* **58**, 1319 (2003).
 - [5] Ch. Froese Fischer and Yu. Ralchenko (unpublished).
 - [6] H. M. S. Blackford and A. Hibbert, *At. Data Nucl. Data Tables* **58**, 101 (1994).
 - [7] U. Griesmann, J. Musielok, and W. L. Wiese, *J. Opt. Soc. Am. B* **14**, 2204 (1997).
 - [8] J. A. Del Val, J. A. Aparicio, V. R. Gonzalez, and S. Mar, *J. Phys. B* **34**, 2513 (2001).
 - [9] S. Djenize, V. Milosavljevic, and M. S. Dimitrijevic, *Astron. Astrophys.* **382**, 359 (2002).
 - [10] K. Danzmann, M. Günther, J. Fischer, M. Kock, and M. Kühne, *Appl. Opt.* **27**, 4947 (1988).
 - [11] K. E. Donnelly, P. J. Kindlmann, and W. R. Bennett, Jr., *IEEE J. Quantum Electron.* **QE-10**, 848 (1974).
 - [12] A. Denis, *C. R. Acad. Sci., Ser. B* **268**, 383 (1969).
 - [13] A. Denis, P. Ceyzeriat, and M. Dufay, *J. Opt. Soc. Am.* **60**, 1186 (1970).
 - [14] J. H. Brand, C. L. Cocke, B. Curnutte, and C. Swenson, *Nucl. Instrum. Methods* **90**, 63 (1970).
 - [15] F. J. Coetzer, P. B. Kotze, and P. van der Westhuizen, *Nucl. Instrum. Methods Phys. Res.* **202**, 19 (1982).
 - [16] K. Blagoev and K. Stankova, *J. Quant. Spectrosc. Radiat. Transf.* **35**, 483 (1986).
 - [17] K. B. Blagoev, E. N. Borisov, and M. L. Burshtein, *Opt. Spektrosk.* **67**, 601 (1989).
 - [18] J. E. Hesser, *Phys. Rev.* **174**, 68 (1968).
 - [19] C. E. Head and M. E. M. Head, *Phys. Rev. A* **2**, 2244 (1970).
 - [20] P. Martin and J. Campos, *Physica B & C* **92**, 147 (1977).
 - [21] P. Martin and J. Campos, *J. Quant. Spectrosc. Radiat. Transf.* **30**, 131 (1983).
 - [22] U. Fink, S. Bashkin, and W. S. Bickel, *J. Quant. Spectrosc. Radiat. Transf.* **10**, 1241 (1970).
 - [23] M. B. Das, *J. Quant. Spectrosc. Radiat. Transf.* **50**, 561 (1993).
 - [24] M. B. Das, *Z. Phys. D: At., Mol. Clusters* **39**, 257 (1997).